PHYSICAL REVIEW C **76**, 061302(R) (2007)

Inverse-kinematics one-proton pickup with intermediate-energy beams: The ^{9}Be (^{20}Ne,^{21}Na + γ)X reaction

A. Gade,[1,2] P. Adrich,[1] D. Bazin,[1] M. D. Bowen,[1,2] B. A. Brown,[1,2] C. M. Campbell,[1,2] J. M. Cook,[1,2] T. Glasmacher,[1,2] K. Hosier,[3] S. McDaniel,[1,2] D. McGlinchery,[3] A. Obertelli,[1] L. A. Riley,[3] K. Siwek,[1,2] J. A. Tostevin,[4] and D. Weisshaar[1]

[1]*National Superconducting Cyclotron Laboratory, Michigan State University, East Lansing, Michigan 48824, USA*

[2]*Department of Physics and Astronomy, Michigan State University, East Lansing, Michigan 48824, USA*

[3]*Department of Physics and Astronomy, Ursinus College, Collegeville, Pennsylvania 19426, USA*

[4]*Department of Physics, Faculty of Engineering and Physical Sciences, University of Surrey, Guildford, Surrey GU2 7XH, United Kingdom*

(Received 5 September 2007; published 5 December 2007)

The possibility of studying particle-like states near the Fermi surfaces of exotic nuclei by using measurements of heavy-ion-induced single-nucleon pickup reactions with in-flight separated rare-isotope beams is discussed. The analysis of an exploratory data set for the intermediate-energy ^{9}Be(^{20}Ne,^{21}Na)X proton pickup reaction measured using a ^{20}Ne beam at 63 MeV per nucleon is reported. The data are compared with expectations based on model calculations of the transfer reaction cross sections and the ^{21}Na residue spectroscopy prediction by the *sd*-shell model. The measured cross sections are broadly consistent with these expectations.

DOI: 10.1103/PhysRevC.76.061302 PACS number(s): 24.50.+g, 25.60.Je, 25.70.Hi, 27.30.+t

Introduction. Both novel and established direct nuclear reaction tools are vital for investigations of the one- and two-nucleon behavior in nuclear many-body systems. By using sufficiently energetic collisions of a projectile and a target nucleus, one, two, or a cluster of nucleons can be removed, excited, or transferred *directly* between the participating nuclei in surface-dominated, grazing collisions. Such reactions involve only a few degrees of freedom and so avoid the full, many-body complications that arise from the formation of a highly excited intermediate compound system. Observables from such direct reactions provide information on the overlaps between the many-body wave functions of the projectile (and target) and the final states of the residual nuclei. Classic examples of direct reactions used to probe the states of single nucleons (and the single-nucleon overlap functions) are the light-ion-induced transfer reactions, e.g., $^{A}Z(d,p)^{A+1}Z$ and $^{A}Z(p,d)^{A-1}Z$. These have been studied over a wide range of incident energies. Whereas the former reaction deposits a neutron onto the ^{A}Z system, thus populating particle-like states at and above the Fermi surface, the latter removes a neutron and so selectively populates hole-like configurations in the residue.

Unstable nuclei with extreme neutron-to-proton ratios have become one major focus of nuclear structure research. Today, many of the most exotic nuclei are produced by fast projectile fragmentation. The exotic nuclei of interest are thus available for experiments as secondary ion beams, typically with $v/c \geqslant 0.3$, necessitating experiments in inverse kinematics. The fast heavy-ion projectiles allow the use of thick reaction targets leading to very forward-focused residues that are detected with high efficiency. Viable in-beam experiments are thus feasible with just a few such ions per second. This use of thick targets, to compensate for low intensity, means that γ-ray detection replaces particle spectroscopy for identifying the final states of the reaction residues.

This basic efficacy of fast fragmentation beams has prompted the development of new direct reactions to probe rare nuclei. One-nucleon removal reactions, e.g., ^{9}Be($^{A}Z,^{A-1}[Z-1]$)X, have been developed into one such novel spectroscopic tool [1]. However, the reactions remove a nucleon from the projectile ground state and therefore selectively populate single-hole configurations in the (mass $A-1$) reaction residues. In these reactions, quantitative nuclear structure information is extracted by comparisons of the measured cross sections with those predicated by the shell model and reaction theory. The latter exploits—because of the high beam energies—the sudden and eikonal approximations [1,2]. As well as being an excellent probe of the structures of halo nuclei (e.g., Ref. [3]) the knockout reaction measurements have (i) observed strong nucleon-nucleon (NN) correlation effects missing from shell-model-like effective-interaction theories [4,5] and (ii) contributed very significantly to mapping the evolution of shell structure, the disappearance of familiar magic numbers, and the formation of new shell gaps in nuclei with extreme N/Z ratios, e.g., Refs. [6–10].

Here we explore a complementary reaction, single-nucleon *pickup* from a light target onto a fast projectile beam. Specifically, we consider proton-pickup reactions on a thick ^{9}Be target. The extent to which the final state of the target-like residue is determined will be discussed later. Potentially, this pickup mechanism could complement knockout studies through the selective population of single particle-like configurations in the mass $A+1$ residues. In the following we therefore make an initial assessment of this feasibility using first available measurements of the proton pickup reaction ^{9}Be(^{20}Ne,^{21}Na)X at 63.4 MeV/nucleon. We apply a distorted-waves (DW) and shell-model theoretical description. The ground state proton separation energy from ^{9}Be is $S_p = 16.89$ MeV and therefore breakup effects (as they arise for example in (d,n) proton transfer) need not enter our present discussion. In addition, because ^{9}Be has no bound excited states, inelastic excitation of the target can be assumed to be included in the (highly) absorptive ^{20}Ne + ^{9}Be optical interaction.

Previous studies of proton *particle*-like states have been the realm of (d,n) and (^{3}He, d) light-ion-induced transfer reactions on stable targets carried out in normal kinematics.

Low-energy (of order 10 MeV/u) heavy-ion-induced transfer reactions have proven to be valuable for spectroscopic studies of stable nuclei (e.g., Ref. [11]), also revealing a selectivity toward high-j single-particle orbitals [12]. The momentum distributions of projectile-like fragments in heavy-ion-induced pickup reactions produced at projectile energies above 80 MeV/nucleon have been studied [13] and spin-polarized exotic beams have been produced using single-nucleon pickup at 150 MeV/nucleon [14]. Programs are also emerging to perform barrier-energy heavy-ion transfer experiments with exotic beams [15]. With reference to our chosen reaction, ^{9}Be(^{20}Ne,^{21}Na), low-energy analyses of (d, n) and (^{3}He, d) reaction data on a ^{20}Ne target are also available, most recently in Refs. [16] and [17], respectively. These analyses are in reasonable agreement with the sd-shell model, discussed here in the context of the present intermediate-energy measurements.

Generic considerations of linear (and angular) momentum matching in particle-transfer reactions at higher collision energies favor the use of targets in which the transferred nucleon is more deeply bound [18,19]. For example, the (α, t) reaction was used at RIKEN to study proton configurations in neutron-rich ^{23}F, using the α(^{22}O,^{23}F) reaction at 63 MeV per nucleon [20,21]. The ^{9}Be target of the present work also provides such well-bound protons (with $S_p = 16.89$ MeV) but avoids experimental complications arising from the use of a gas target. At energies of order 60 MeV/nucleon and greater, the linear and angular momentum matching for single-nucleon transfer is not optimal [18] for maximizing the yield for transfer of nucleons into the available low-ℓ, bound sd-shell states in ^{21}Na. Rather, we depend upon the strong binding and extended momentum distribution of the transferred proton in the ^{9}Be target to generate a sufficiently extended higher energy tail to the transfer yield to make the pickup cross section measurements feasible, typically of order 1 mb. See also Ref. [21].

Experiment and results. The ^{20}Ne secondary beam of the present experiment was produced by fragmentation of a 150 MeV per nucleon ^{36}Ar primary beam, delivered by the Coupled Cyclotron Facility of the National Superconducting Cyclotron Laboratory, onto a 893 mg/cm^2 ^{9}Be production target. The ions of interest were selected in the A1900 fragment separator [22], which was operated at 0.5% momentum acceptance. The ^{20}Ne secondary beam was then incident on a 188(4) mg/cm^2 thick ^{9}Be reaction target positioned at the focus of the large-acceptance S800 spectrograph [23]. The reaction residues were identified on an event-by-event basis from the time of flight taken between two scintillators, the energy loss was measured in the ionization chamber, and the position and angle information was provided by the cathode readout drift chambers of the S800 focal-plane detector system [23] (see Fig. 1). The longitudinal momentum distributions of the unreacted ^{20}Ne beam and of the ^{21}Na one-proton pickup residues were obtained from trajectory reconstruction [24].

An inclusive cross section of 1.85(12) mb was measured for the ^{9}Be(^{20}Ne,^{21}Na)X one-proton pickup reaction based on the yield of ^{21}Na reaction residues divided by the number of incoming ^{20}Ne projectiles relative to the number density of the reaction target. Systematic uncertainties of 4 and 2% were attributed to the stability of the incoming beam and the choice of the software gates, respectively. These were assumed to be independent and were added in quadrature to the statistical uncertainty.

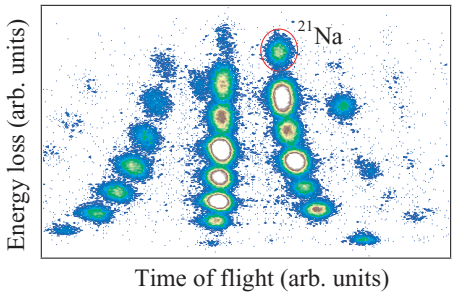

FIG. 1. (Color online) Identification of the ^{20}Ne + ^{9}Be projectile-like reaction residues in the S800 focal plane, shown as the energy loss measured in the ionization chamber versus the ion's time of flight. The ^{21}Na one-proton pickup residues are clearly separated from the other reaction residues.

The secondary ^{9}Be target was surrounded by SeGA, an array of 32-fold segmented HPGe detectors [25]. Sixteen detectors were arranged in two rings (with 90° and 37° central angles with respect to the beam axis). The 37° ring was equipped with seven detectors and the 90° ring with nine detectors. The photo-peak efficiency of the array was measured with ^{152}Eu and ^{226}Ra calibration standards and corrected for the Lorentz boost of the γ-ray distribution emitted by nuclei moving with $v/c \approx 0.3$.

In coincidence with the ^{21}Na one-proton pickup residues detected in the S800, γ-ray transitions at 330(3) keV and 1382(4) keV and around 2420 keV were detected in SeGA (see Fig. 2). Three ^{21}Na excited states are known below its proton separation energy $S_p = 2.43$ MeV (see inset of Fig. 2). The 330 keV transition depopulates the first excited $5/2^+$ state to the $3/2^+$ ground state. The 1382 keV transition corresponds to the decay from the first excited $7/2^+$ state to the $5/2^+$ level and a 2424 keV γ decay connects the first excited $1/2^+$ state and the ground state. For the $7/2^+$ state, a 7.5(33)% branch to the ground state has been reported but could not be observed in the present experiment.

From the γ-ray branching ratios and the level scheme of ^{21}Na, the cross sections for the one-proton pickup to individual ^{21}Na final states were deduced from an input-output balance. The $5/2^+$ state is populated the strongest at 86(6)%. All other states are much less fed by the reaction. The cross section for the pickup to the $7/2^+$ level was corrected for the 7.5% branch to the ground state reported in the literature. For the $1/2^+$ state just below the proton separation energy, an upper limit for the cross section was derived. The population of the ground state was obtained by subtraction and found to be consistent with zero, with an upper limit of 0.06 mb. In the laboratory frame, a γ-ray transition was detected at 981 keV (see Fig. 2) and is attributed to population of the only bound excited state, ^{8}Li(1^+), of the target residue. The cross section to this final state is 0.13(4) mb. The experimental results are summarized in Table I.

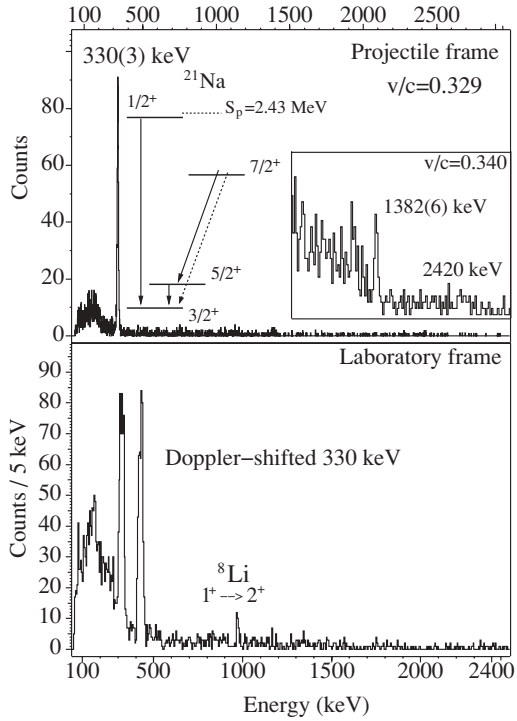

FIG. 2. (Upper panel) Doppler-reconstructed γ-ray spectrum in coincidence with ^{21}Na. The most intense photo-peak detected in SeGA corresponds to the $5/2^+ \rightarrow 3/2^+$ 332 keV deexcitation γ ray. The $5/2^+$ excited state is long-lived and the 332 keV γ ray is emitted predominantly after the ^{9}Be target with $v/c = 0.329$. (Lower panel) γ-ray spectrum in coincidence with ^{21}Na as detected in the laboratory frame.

Discussion. For a first analysis of the present data, transfer reaction calculations were performed using the post form of the finite-range distorted waves Born approximation (DWBA) using the direct reactions code FRESCO [27]. A one-step proton transfer was assumed from ^{9}Be in the initial state and, in all channels, the final states were assumed to be two-body. The ^{9}Be(^{20}Ne,^{21}Na)X reaction was thus assumed to be dominated by direct transfer processes calculated as $^{20}\text{Ne}(^9\text{Be}, ^8\text{Li}(I^+))^{21}\text{Na}(j^\pi)$ at 63.4 MeV per nucleon incident energy. In these calculations the highly absorptive nuclear parts of the $^{20}\text{Ne} + ^9\text{Be}$ and $^{21}\text{Na} + ^8\text{Li}$ interactions were assumed to be identical. These were calculated, as in recent nucleon knockout reaction studies, by double folding the neutron and proton densities in ^{20}Ne (from Hartree-Fock calculations) and in ^{9}Be (assumed Gaussian with rms radius of 2.36 fm) with an effective NN interaction [2]. The target-like, $[^8\text{Li}(I^+) \otimes \Phi_j]_{3/2^-}$, and projectile-like, $[^{20}\text{Ne}(0^+) \otimes \phi_j]_j$, proton-core relative motion wave functions (overlaps) Φ_j and ϕ_j were treated as follows.

The $^{21}\text{Na}(j^+)$ states were calculated in real Woods-Saxon potentials with radius and diffuseness parameters $r_0 = 1.25$ fm and $a_0 = 0.7$ fm. A spin-orbit interaction of 6 MeV and the same geometry parameters were added. The $5/2^+$ (0.332 MeV) and $1/2^+$ (2.424 MeV) bound states used the physical separation energies. For the relatively narrow $5/2^+$ (4.294 MeV) and $3/2^+$ (4.468 MeV) proton-unbound states two continuum bins were constructed that include the full strength of the resonances, the real potential depths being adjusted so that the $5/2^+$ and $3/2^+$ $p + ^{20}$Ne phase shifts passed through $\pi/2$ at the appropriate center of mass energies. The cross section to each of the ^{21}Na final states is scaled by the shell-model spectroscopic factors, C^2S.

Our $^9\text{Be}(3/2^-)$ to $^8\text{Li}(I^+)$ overlaps use the Variational Monte Carlo (VMC) overlaps and their associated spectroscopic amplitudes of Wiringa *et al.* [28]. For convenience, the tabulated numerical $I^\pi = 1^+(-0.403 \times 1p_{3/2}$ and $0.456 \times 1p_{1/2})$, $I^\pi = 2^+(0.759 \times 1p_{3/2}$ and $0.393 \times 1p_{1/2})$, and $I^\pi = 3^+(0.480 \times 1p_{3/2})$ channel overlaps were each fitted by scaling the normalized $1p_{3/2}$ and $1p_{1/2}$ radial wave

TABLE I. Experimental results are compared to the reaction theory and shell-model calculations. Given are the spin, parity, and excitation energy of the final state and the experimental cross section σ_f for the direct population of this level of ^{21}Na in the pickup reaction. Cross sections are compared to the reaction theory calculations, the single-particle cross section σ_{sp}, the corresponding ^{20}Ne to ^{21}Na spectroscopic factor from the USD shell model [26], the resulting total cross section for the population of the final state σ_f^{th}, and the cross section broken down into the population of different final states of the ^{8}Li target residue.

J^π	E (keV)	σ_f expt. (mb)	σ_{sp} sum (mb)	C^2S SM	σ_f^{th} tot. (mb)	σ_f^{th} ^{8}Li$_{2^+,3^+}$ (mb)	σ_f^{th} ^{8}Li$_{1^+}$ (mb)
$3/2^+$	0.0	<0.06	–	–	–	–	–
$5/2^+$	331	1.59(15)	3.05	0.63	1.92	1.49	0.436
$7/2^+$	1716	0.20(5)	–	–	–	–	–
$1/2^+$	2424	⩽0.12(1)	0.028	0.65	0.018	0.013	0.005
			Above the proton separation energy $S_p = 2.43$ MeV				
$5/2^+$	4294	–	1.69	0.123	0.21	0.163	0.048
$3/2^+$	4468	–	0.97	0.294	0.28	0.178	0.104
σ (mb)							
	to bound states in ^{21}Na						
σ_{inc}		1.85(12)			1.94		
$\sigma(^8\text{Li};1^+)$		0.13(4)			0.44		

functions calculated in different Woods-Saxon potentials. These fitted potentials and the VMC spectroscopic amplitudes were then used for the binding and transfer interactions in FRESCO. Thus, while in the present study we examine the USD shell-model spectroscopic factors C^2S [26] in the context of the ^{21}Na(j^+) final state yields, it should be noted that these VMC amplitudes and ^{9}Be to ^{8}Li(I^π) radial overlaps are implicit in the calculations presented.

In Table I the experimental results are compared to the calculations outlined above. The pattern of the measured populations of the known ^{21}Na particle-like bound states, in particular the observed dominance of the $5/2^+$ state and the vanishing population to the ground state, is in good agreement with the (d, n) [16] and $(^3\mathrm{He}, d)$ [17] light-ion reaction analyses. Population of the $7/2^+$ (1.72 MeV) state, observed with low yields in the light-ion and the present heavy-ion experiments, is indicative of a higher-order process. Such excitations, described quantitatively in Ref. [16] by including the ^{20}Ne(2^+, 1.63 MeV) inelastic channel, and $[^{20}\mathrm{Ne}(2^+) \otimes \phi_j]_{7/2}$ transfers, can be included in the future. Our emphasis here is on the known single-particle-like configurations. The $5/2^+$ (4.294 MeV) and $3/2^+$ (4.468 MeV) proton-unbound excited states are also predicted to be populated in the reaction, but are unobserved here in γ spectroscopy.

Thus, the overall magnitude of the inclusive cross section and the population pattern to individual ^{21}Na(j^+) final states are well reproduced when combining the DWBA model and the spectroscopic factors C^2S from the USD shell model. This gives promise that the reaction mechanism may indeed have the potential to locate dominant single-particle-like strength using fast rare isotope beams. We note however that, from this analysis, there is a significant deviation of the measured and calculated cross sections for the transfer to the ^{8}Li(1^+) excited state, which the calculations overestimate. The amplitudes of the target overlaps for this 1^+ configuration enter through the VMC values, discussed above. Such details of the distribution of the final state yields with respect to the target-like residues cannot be addressed with the present data set. Additional data, using different projectiles and targets (e.g., ^{12}C) will be necessary to understand this target-like residue distribution. It will also be very valuable to determine the extent to which details of the target structures (and target-like final state yields) affect the cross section distributions to the final states of the heavy pickup residues. This dependence could be rather weak in the case of such poorly linear and angular momentum matched reactions.

The measured inclusive longitudinal momentum distribution of the ^{21}Na pickup residues and that of the unreacted ^{20}Ne projectile beam after passage through the target are shown in Fig. 3. The measured ^{21}Na residue distribution is narrow compared to typical momentum distributions from one-nucleon knockout reactions and thus strongly supports the direct nature of the pickup reaction. As one would expect, the ^{21}Na parallel momentum distribution is broadened compared to that of the unreacted ^{20}Ne as a result of the differential momentum loss from the pickup reactions taking place toward the front or the back of the ^{9}Be reaction target, resulting in a rectangular distribution of width 0.13 GeV/c.

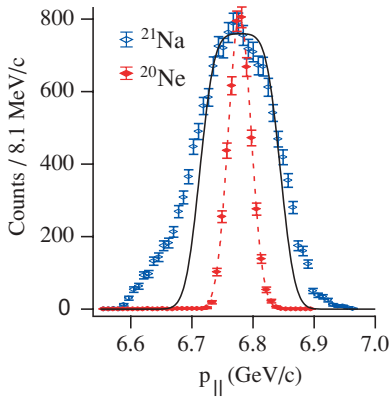

FIG. 3. (Color online) Measured longitudinal momentum distributions of the ^{21}Na one-proton pickup residues and of the unreacted ^{20}Ne beam having passed through the target. The solid curve is the predicted distribution based on two-body direct reactions and is the result of the convolution of the unreacted ^{20}Ne distribution and the differential energy loss of the ^{21}Na residues in the reaction target.

Given the assumed two-body nature of the $^8\mathrm{Li} + ^{21}\mathrm{Na}$ final states, the intrinsic transfer reaction $d\sigma/dp_\parallel$ distributions are very narrow compared to those discussed above. Explicitly, if the particles in the final state are 3 and 4, and labels 1 and 3 refer to the heavy projectile and the projectile-like residue, respectively,

$$\frac{d\sigma}{dp_\parallel} = \frac{2\pi}{p_3}\left\{\frac{m_3}{(m_3+m_4)}\frac{p_1}{p_3}\cos\theta_L - 1\right\}\frac{d\sigma}{d\Omega_L}, \qquad (1)$$

where $d\sigma/d\Omega_L$ is the transfer reaction differential cross section in the laboratory frame and p_3 the residue momentum at the laboratory angle θ_L. The Q values are also all sufficiently similar that there is essentially no broadening when adding the different final state contributions. Thus, the shape of the expected momentum distribution is the convolution of the differential energy loss and the unreacted ^{20}Ne profile. This is shown by the solid curve in Fig. 3, to be compared with the ^{21}Na distribution. The width is in reasonable agreement with the measured distribution, but there are indications, from the tails on the experimental distribution, of small contributions from other than the two-body final states assumed in the present reaction dynamics treatment, such as our approximate treatment of the unbound ^{8}Li(3^+) excited state.

Unlike in knockout reaction measurements, the pickup residue momentum distribution is not expected to contain spectroscopic information. Nevertheless, it is shown to have useful diagnostic value for our understanding of the reaction mechanism, e.g., the possible importance of missing target-like channels that lead to more complex (few-body) final states.

Summary. In summary, we have investigated an example of an inverse kinematics, $(^AZ, ^{A+1}[Z+1])$ proton pickup reaction on a ^{9}Be target as a possible tool for the study of particle-like structures in exotic nuclei that are available only as low-intensity, fast fragmentation beams. The results for a ^{20}Ne beam of 63 MeV per nucleon were found to be consistent with distorted waves transfer reaction and shell-model theory. The measured residue momentum distribution is narrow and

is strongly supportive of the direct nature of the mechanism underlying the measured pickup reaction events.

Outstanding details of the distribution of the final state yields with respect to the target-like residues will require additional data, ideally using different projectiles and targets. The extent to which details of the target structures affect the cross section distributions to the final states of the heavy exotic pickup residues of interest can then be examined.

The pattern of the observed population of the specific ^{21}Na final states yields nuclear structure information in line with the predictions of shell-model calculations and verifies that the reaction mechanism (i) can be accessed with current experimental tools and (ii) could be a very significant complementary spectroscopic technique for the spectroscopy of particle states in the most exotic systems. Because this reaction mechanism favors the population of single-particle states with high orbital angular momentum, it will be well suited to identify $\ell = 3$ intruder states in the vicinity of the "island of inversion" [29] and aid in the quest to unravel new exotic regions in the nuclear chart where high-ℓ intruder orbitals descend across shell gaps and significantly modify the nuclear structure as established for stable nuclei.

We acknowledge valuable discussions with B. M. Sherrill. This work was supported by the National Science Foundation under Grants PHY-0606007 and PHY-0555366 and by the United Kingdom Science and Technology Facilities Council (STFC) under Grant EP/D003628.

[1] P. G. Hansen and J. A. Tostevin, Annu. Rev. Nucl. Part. Sci. **53**, 219 (2003).
[2] J. A. Tostevin, G. Podolyák, B. A. Brown, and P. G. Hansen, Phys. Rev. C **70**, 064602 (2004); J. A. Tostevin and B. A. Brown, Phys. Rev. C **74**, 064604 (2006).
[3] T. Aumann *et al*., Phys. Rev. Lett. **84**, 35 (2000).
[4] B. A. Brown, P. G. Hansen, B. M. Sherrill, and J. A. Tostevin, Phys. Rev. C **65**, 061601(R) (2002).
[5] A. Gade *et al*., Phys. Rev. Lett. **93**, 042501 (2004).
[6] A. Navin *et al*., Phys. Rev. Lett. **85**, 266 (2000).
[7] J. R. Terry *et al*., Phys. Lett. **B640**, 86 (2006).
[8] A. Gade *et al*., Phys. Rev. C **71**, 051301(R) (2005).
[9] J. Fridmann *et al*., Phys. Rev. C **74**, 034313 (2006).
[10] A. Gade *et al*., Phys. Rev. C **74**, 047302 (2006).
[11] D. G. Kovar *et al*., Phys. Rev. C **17**, 83 (1978).
[12] P. D. Bond, J. Barrette, C. Baktash, C. E. Thorn, and A. J. Kreiner, Phys. Rev. Lett. **46**, 1565 (1981).
[13] G. A. Souliotis, D. J. Morrissey, N. A. Orr, B. M. Sherrill, and J. A. Winger, Phys. Rev. C **46**, 1383 (1992).
[14] D. E. Groh *et al*., Phys. Rev. Lett. **90**, 202502 (2003).
[15] D. C. Radford *et al*., Nucl. Phys. **A752**, 164c (2005).
[16] A. Terakawa *et al*., Phys. Rev. C **48**, 2775 (1993).
[17] A. M. Mukhamedzhanov *et al*., Phys. Rev. C **73**, 035806 (2006).
[18] D. M. Brink, Phys. Lett. **B40**, 37 (1972).
[19] W. R. Phillips, Rep. Prog. Phys. **40**, 345 (1977).
[20] S. Michimasa *et al*., Phys. Lett. **B638**, 146 (2006).
[21] S. Shimoura, J. Phys. G: Nucl. Part. Phys. **31**, S1759 (2005).
[22] D. J. Morrissey *et al*., Nucl. Instrum. Methods Phys. Res. B **204**, 90 (2003).
[23] D. Bazin *et al*., Nucl. Instrum. Methods Phys. Res. B **204**, 629 (2003); J. Yurkon *et al*., Nucl. Instrum. Methods Phys. Res. A **422**, 291 (1999).
[24] M. Berz, K. Joh, J. A. Nolen, B. M. Sherrill, and A. F. Zeller, Phys. Rev. C **47**, 537 (1993).
[25] W. F. Mueller *et al*., Nucl. Instrum. Methods A **466**, 492 (2001).
[26] B. A. Brown and B. H. Wildenthal, Annu. Rev. Nucl. Part. Sci. **38**, 29 (1988).
[27] I. J. Thompson, Computer code FRESCO. Available at http://www.fresco.org.uk/index.htm; see also I. J. Thompson, Comput. Phys. Rep. **7**, 167 (1988).
[28] R. W. Wiringa *et al*. (private communication). The configuration and momentum space overlaps are available at http://www.phy.anl.gov/theory/research/overlap/.
[29] E. K. Warburton, J. A. Becker, and B. A. Brown, Phys. Rev. C **41**, 1147 (1990).